



7th International Conference on Silicon Photovoltaics, SiliconPV 2017

High-throughput front and rear side metallization of silicon solar cells using rotary screen printing

Andreas Lorenz^a, Anna Münzer^a, Martin Lehner^b, Roland Greutmann^c, Heinz Broucker^c, Holger Reinecke^d, Florian Clement^a

^aFraunhofer Institute for Solar Energy, Heidenhofstr. 2, 79110 Freiburg, Germany

^bLehner Engineering GmbH, Ebnestrasse 18, 9032 Engelburg, Switzerland

^cGallus Ferd. Rüesch AG, Harzbüchelstrasse 34, 9016 St. Gallen, Switzerland

^dAlbert-Ludwigs-Universität, Institut für Mikrosystemtechnik, Georges-Köhler-Allee 101, 79110 Freiburg, Germany

Abstract

Rotational screen printing (RSP) has recently attracted attention as a highly promising high-throughput alternative for the metallization of Silicon solar cells. Compared to other metallization approaches, RSP is already a well-developed printing method which has been used for various industrial applications during the last decades. The unique benefit of this technology is the ability to apply a thick film metallization combined with a high throughput. Within the present work, we will discuss the actual achievements and challenges of this approach. We show the results of Aluminium back surface solar cells with a RSP rear side metallization and a mean conversion efficiency of $\eta = 19.4\%$ compared to reference solar cells with flatbed screen printed rear side metallization and a conversion efficiency of $\eta = 19.3\%$. We further investigate the properties of fine line cylinder screens used for RSP and conventional flatbed screen printing. Using RSP with a fine line cylinder screen, we printed contact fingers with a mean width down $w_f = 61\ \mu\text{m}$. Finally, we discuss the path to a further optimization of this highly promising approach.

© 2017 The Authors. Published by Elsevier Ltd.

Peer review by the scientific conference committee of SiliconPV 2017 under responsibility of PSE AG.

Keywords: Silicon Solar Cells; Metallization; Rotational Printing; Rotary Screen Printing

1. Introduction

Today, flatbed screen printing (FSP) is the state-of-the-art technology for solar cell metallization. However, the throughput of a single FSP metallization line is currently limited to approx. 2000 wafers/h [1]. A highly promising route to considerably increase throughput is the usage of rotational printing methods. Such methods can realize an

expected throughput of at least 6000 wafers/h on a single metallization line. However, new metallization approaches can only compete with flatbed screen printing technology under certain preconditions: they have to be fast, reliable, easy-to-handle and must avoid a cost-intensive development of new consumables. Rotary screen printing (RSP) is a well-established and highly developed printing technology [2,3] which is able to combine these benefits.

To date, this technology is primarily used on web-based materials (i.e. label or textile printing [7]) with a printing speed of up to 100 m/min. Similar to flatbed screen printing, a woven screen mesh covered with a partly open emulsion layer is used as printing form. However, in contrary to the flat screen used in FSP, cylinder-shaped screens are used for RSP. The meshes of such screens consist of up to 400 wires per inch (mesh count). Due to stability reasons of the cylinder screen, the wires of the mesh are significantly thicker compared to flat screens (Fig. 1). FSP requires two printing sequences. Firstly, the open areas of the screen are filled using a metal flood bar. Secondly, the paste is pressed through the openings of the flat screen using a flexible squeegee. Within the RSP process, the paste is constantly pressed through the screen openings by a fixed squeegee within the rotating screen cylinder (Fig. 2). A pre-filling of the screen is thus not necessary. RSP requires a lower paste viscosity compared to FSP pastes to ensure a good paste transfer through the screen openings [3]. The ability to transfer thick film metallization patterns makes RSP interesting for both – front and rear side metallization of c-Si solar cells.

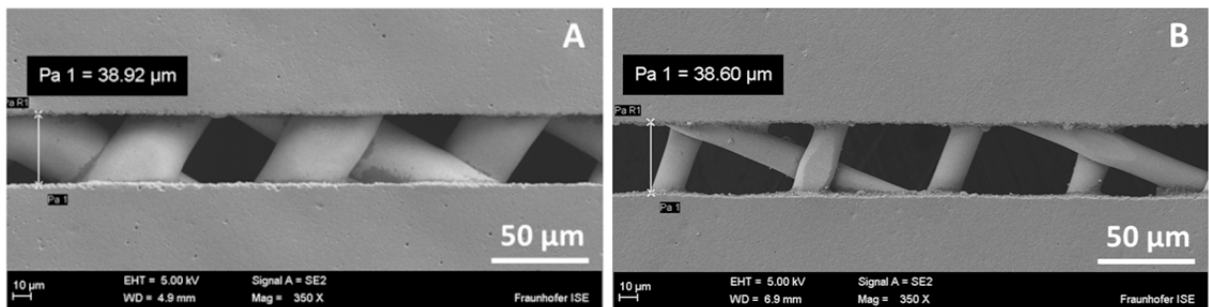


Fig. 1. SEM image of a fine line contact finger opening within a rotary screen (A) and a flatbed screen (B). The significantly greater thread thickness of the rotary screen mesh ($d_{RSP} = 28 \mu\text{m}$) compared to the flatbed screen mesh ($d_{FSP} = 18 \mu\text{m}$) is clearly visible.

First attempts to use this technology for solar cell metallization date back to the year 1999, however no results are known from these activities [4]. Results of a first pre-test have been published recently [3]. Within this work, we provide a detailed investigation of the paste rheology and the metallization results of RSP on the front side in comparison to reference cells using flatbed screen printing. The results can be regarded as a starting point for the further development of this highly interesting metallization approach.

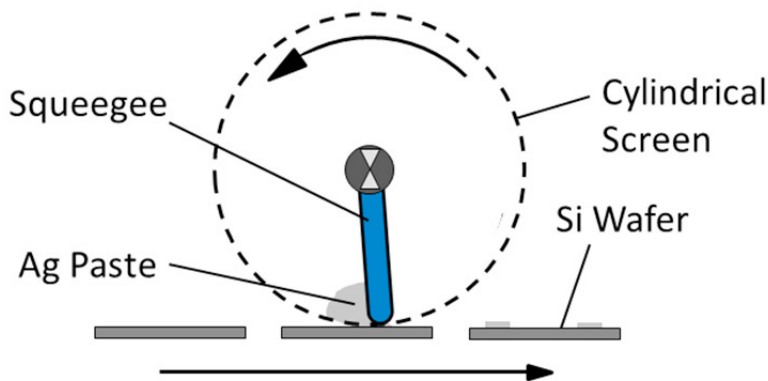


Fig. 2. Schematic view of a rotary screen printing unit for solar cell metallization

Nomenclature

A_f	Mean finger cross-section area	$[\mu\text{m}^2]$
$d_{\text{Al,FFO}}$	Layer thickness of Al rear side metallization after contact firing	$[\mu\text{m}]$
d_w	Wire diameter	$[\mu\text{m}]$
FF	Fill factor	$[\%]$
h_f	Mean finger height	$[\mu\text{m}]$
j_{sc}	Short-circuit current density	$[\text{mA}/\text{cm}^2]$
R_L	Lateral finger resistance	$[\Omega/\text{cm}]$
R_{SH}	Emitter sheet resistance	$[\Omega/\text{sq}]$
T	Temperature	$[\text{°C}]$
t_{ALBSF}	Mean depth of Al back surface field	$[\mu\text{m}]$
T_{FFO}	Nominal peak set temperature of the contact firing process	$[\text{°C}]$
V_{oc}	Open-circuit voltage	$[\text{mV}]$
v_p	Printing speed	$[\text{mm}/\text{s}]$
V_{th}	Theoretical paste volume of screen mesh	$[\text{cm}^3/\text{m}^2]$
w_b	Width of busbars	$[\mu\text{m}]$
w_f	Mean finger width	$[\mu\text{m}]$
w_n	Nominal finger width in the digital data	$[\mu\text{m}]$
η	Viscosity	$[\text{Pas}]$
η	Conversion efficiency	$[\%]$
τ_y	Yield stress	$[\text{Pa}]$
$\dot{\gamma}$	Shear rate	$[\text{s}^{-1}]$

2. Experimental setup

2.1. Experimental groups

Fig. 3 shows the experiment plan. The study is divided into two separate experiments. Aim of experiment 1 is a comparison of RSP and FSP technology with respect to the rear side metallization of Al BSF solar cells. Within this experiment, 3 groups with RSP-printed rear side metallization and 1 reference group with FSP-printed rear side metallization have been fabricated. Experiment 2 investigated the ability of RSP to realize the front side metallization of Al BSF solar cells. Within this experiment, 1 group with RSP-printed front side metallization and 1 reference group with FSP-printed front side metallization have been realized.

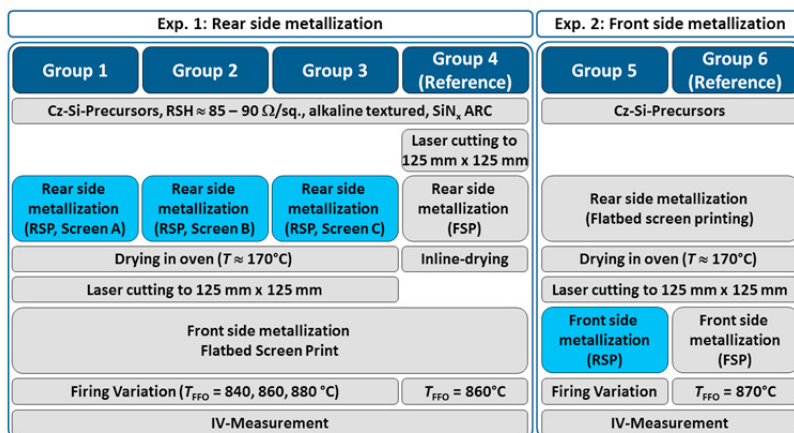


Fig. 3. Experiment plan.

2.2. RSP metallization of Si solar cells

Industrially pre-produced p-type Czochralski-grown Si 6'' wafers (Cz-Si precursors) with an n-type emitter ($R_{SH} \approx 85\text{-}90 \text{ } \Omega/\text{sq.}$) and SiN_x anti-reflection coating have been used for the experiment. A commercial Ag paste for FSP solar cell front side metallization and an Al paste for the rear side metallization have been modified by diluting it to an adequate viscosity for RSP. Rheological parameters (flow curve $\eta(\dot{\gamma})$ and yield stress τ_y) of the adapted pastes have been measured using an Anton Paar MCR101 rotational rheometer. The rotary screen printing metallization has been realized on a Gallus EM 280 label printing machine. This machine is designed to print on continuous web materials like foil or paper web. Every wafer has been fixed individually on the foil web before each print run to enable the transport of the wafers through the rotary screen printing unit. Printing speed has been set to $v_p \approx 330 \text{ mm/s}$. Due to existing challenges with the alignment of the printing layout, a smaller solar cell layout with 125 mm edge length has been printed on precursors with 156 mm edge length. The smaller solar cells (125 mm x 125 mm) have subsequently been cut out along the edge of the printed rear/front side metallization by a laser cutting process.

2.3. Experiment 1: rear side metallization of Al BSF solar cells

Within experiment No. 1, three groups of solar cells with approx. 45 precursors in total have been metallized on the rear side using rotary screen printing (group 1 to 3). As a reference, 20 precursors have been metallized on the rear side using flatbed screen printing (group 4). Group 1 to 3 have been metallized using three different types of rotary screens with different meshes and thus a varying paste transfer volume (Table 1). A standard Al paste has been used after diluting it to an adequate viscosity for RSP. The rear side metallization of the FSP reference group has been carried out on cut-out wafers (125 mm x 125 mm) using a standard flatbed screen (screen mesh count: 280 wires/inch) and the same Al paste without dilution. All wafers have been cured in a cabinet dryer at $T \approx 170^\circ\text{C}$ for 15 min. directly after printing. Subsequently, all wafers were cut down to a format of 125 mm x 125 mm along the edge of the rear side metallization using a laser cutting process. An H-pattern grid layout (85 contact fingers with $w_n = 50 \text{ } \mu\text{m}$ and 3 busbars with $w_b = 1,0 \text{ mm}$) has been printed in one run on all 4 groups using FSP on an ASYS metallization line and a standard Ag paste for front side metallization. A firing variation with 3 temperatures ($T_{\text{FFO1}} = 840 \text{ } ^\circ\text{C}$, $T_{\text{FFO2}} = 860 \text{ } ^\circ\text{C}$, $T_{\text{FFO3}} = 880 \text{ } ^\circ\text{C}$) has been carried out. Finally, the I-V-results of all solar cells have been measured using a JRT Artist cell tester. A profound analysis using scanning electron microscopy (SEM) has been carried out to investigate the thickness of the Al layer on the rear side and the morphology of the Al back surface field (Al BSF) of all groups after contact firing.

Table 1: Specification of rotary and flatbed screens for the experimental groups 1 – 4.

Group	Rear side	Screen mesh count [wires/inch]	Wire diameter d_w [μm]	Theoretical paste volume V_{th} [cm^3/m^2]	Front side	Screen mesh count [wires/inch]	Wire diameter d_w [μm]	Theoretical paste volume V_{th} [cm^3/m^2]
1	RSP	200	53	22	FSP	400	18	16
2	RSP	145	57	32	FSP	400	18	16
3	RSP	88	35	67	FSP	400	18	16
4	FSP	280	25	27	FSP	400	18	16

2.4. Experiment 2: Front side metallization of Al BSF solar cells

Within the second experiment, the potential of RSP for the front side metallization of H-Pattern Al BSF solar cells has been investigated. Therefore, a group with RSP front side metallization (group 5) and a reference group with FSP front side metallization (group 6) have been fabricated. Prior to the printing test, two types of RSP cylinder screens (screen mesh count: 325 wires/inch) with a different emulsion (type A and B) have been realized with a test layout (Table 2). The layout consisted of an H-pattern grid (125 mm x 125 mm) with 75 fingers ($w_n = 35 \mu\text{m}$) and 4 busbars ($w_b = 1,0 \text{ mm}$). Additionally, finger test elements with a nominal width of $w_n = 25 \mu\text{m}$, $w_n = 35 \mu\text{m}$ and $w_n = 45 \mu\text{m}$ have been placed parallel and perpendicular to the direction of printing around the grid layout. The quality of the finger openings within the two types of cylinder screens has been investigated using scanning electron microscopy (SEM). The best cylinder screen (emulsion type A) has been used to print the test pattern on Cz-Si precursors with an edge length of 156 mm using RSP technology and the diluted Ag paste (group 5).

Table 2: Specification of rotary and flatbed screens for the experimental groups 5 and 6.

Group	Front side	Screen mesh count [wires/inch]	Wire diameter d_w [μm]	Theoretical paste volume V_{th} [cm^3/m^2]	Rear side	Screen mesh count [wires/inch]	Wire diameter d_w [μm]	Theoretical paste volume V_{th} [cm^3/m^2]
5	RSP	325	28	14.5	FSP	280	25	27
6	FSP	400	18	16	FSP	280	25	27

A reference group has been realized by printing the same test layout on an ASYS FSP metallization line using a standard flatbed screen (screen mesh count: 400 wires/inch) (group 6). All wafers have been cured in a cabinet dryer at $T \approx 170^\circ\text{C}$ for 15 min. directly after printing. The resulting finger geometry of the RSP- and FSP-printed test layout has been statistically analyzed using confocal microscopy and an image analysis software which has been developed at Fraunhofer ISE [5]. Furthermore, a profound investigation of the finger geometry has been carried out using scanning electron microscopy (SEM). Finally, lateral finger resistance R_L of both groups has been measured using four-point probe measurement.

3. Results and discussion

3.1. Experiment 1: rear side metallization of Al BSF solar cells

First RSP printing tests revealed the necessity to dilute the Al paste to an adequate viscosity to ensure a stable paste transfer. The modified paste showed a viscosity between $\eta = 93.2 \text{ Pas}$ (shear rate $\dot{\gamma} = 0.1 \text{ s}^{-1}$) and $\eta = 3.5 \text{ Pas}$ ($\dot{\gamma} = 1000 \text{ s}^{-1}$) after diluting it with an amount of 5.0 wt% (weight percent) of α -Terpineol. Using the modified Al paste, a visually homogeneous rear side metallization could be realized with all three RSP cylinder screens (group 1 to 3). Depending on the properties of the cylinder screens, a layer thickness between $d_{Al,FFO1} = 20 \mu\text{m}$ and $d_{Al,FFO3} = 40 \mu\text{m}$ after contact firing could be achieved. The FSP reference cells obtained an Al layer thickness of $d_{Al,FFO4} = 24 \mu\text{m}$ after contact firing (Fig. 4). The Al layer of all groups showed a comparable homogeneity with occasional, randomly distributed pinholes (Fig. 5). These pinholes are most likely caused by particle agglomerates or air bubbles within the paste and could also be observed within the FSP rear side metallization layer.

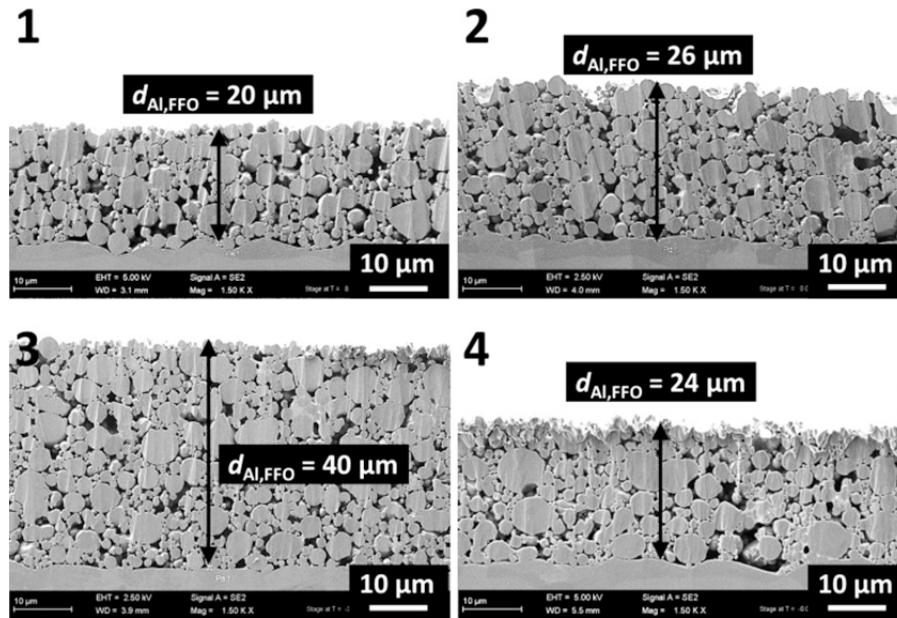


Fig. 4. SEM images of the Al rear side metallization after contact firing for samples of group 1, 2, 3 and 4 (SEM parameters: secondary electron detection, accelerating voltage $V = 2.5 - 5$ KV, working distance $w = 3.1 - 5.5$ mm)..

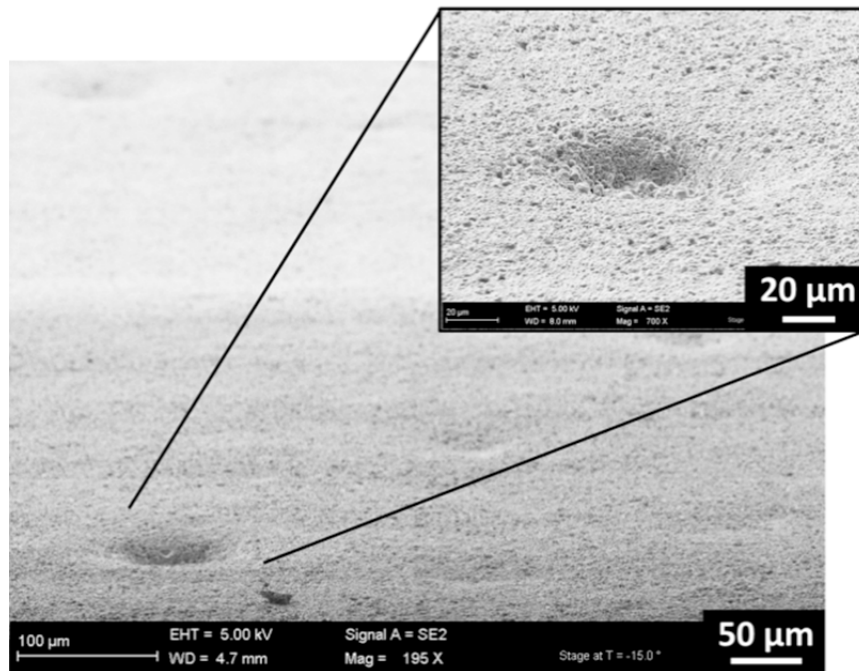


Fig. 5. SEM-Image of the rear side metallization of group 2 /SEM-image of a pinhole within the rear side metallization (SEM parameters: secondary electron detection, accelerating voltage $V = 5.0$ KV, working distance $w = 4.7 - 8.0$ mm).

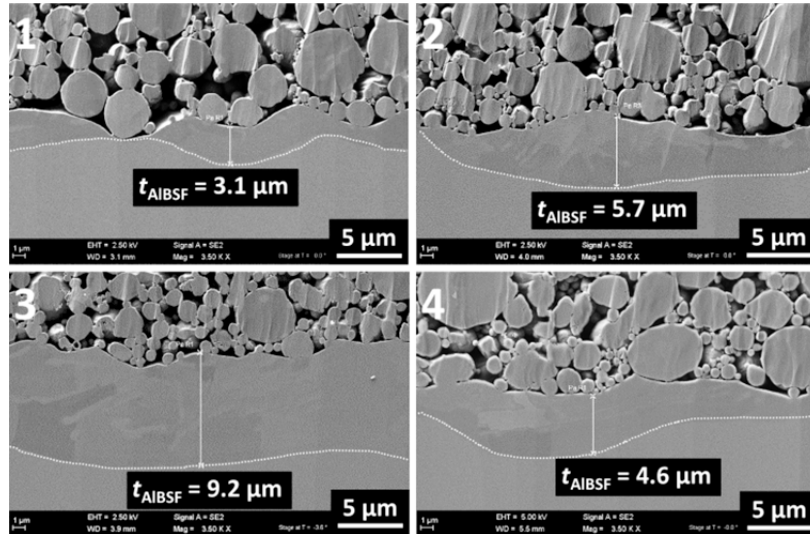


Fig. 6. SEM images of the contact zone between rear side metallization and Si after contact firing. The depth of the Al BSF is indicated by the dashed line (SEM parameters: secondary electron detection, accelerating voltage $V = 2.5 - 5.0$ K V, working distance $w = 3.1 - 5.5$ mm).

Table 3: Thickness of the Al rear side metallization d_{Al} and mean depth t_{ALBSF} of the Al BSF for group 1 to 4 after contact firing.

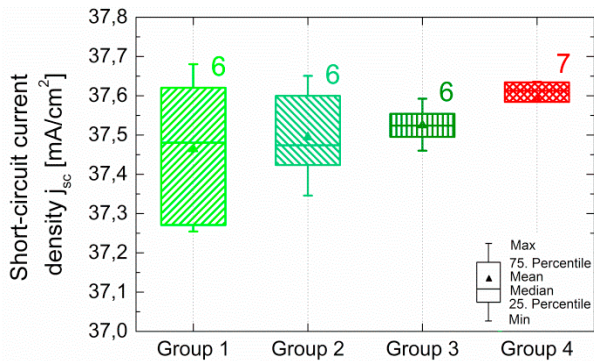
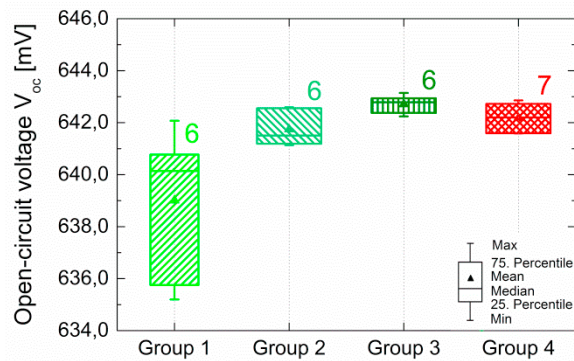
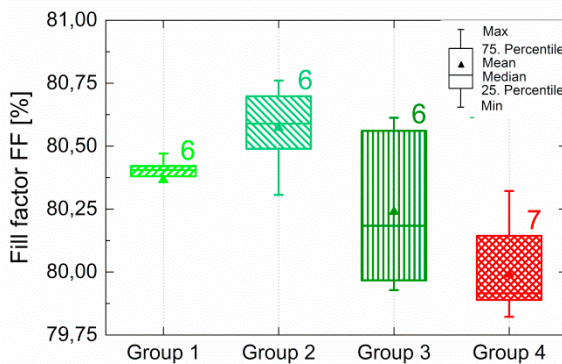
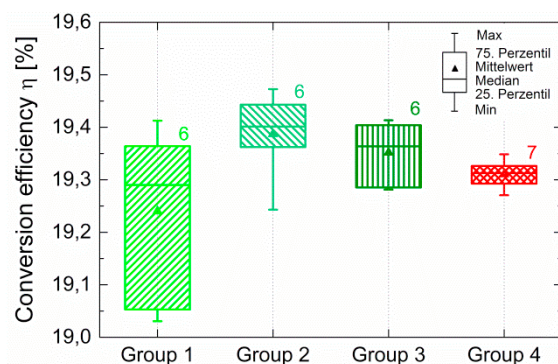
Group	Al layer thickness d_{Al} [μm]	Mean Depth of the AL BSF t_{ALBSF} [μm]
1	20	2.5
2	26	3.6
3	40	7.8
4	24	4.0

A SEM analysis of the resulting Al BSF after contact firing revealed a significant dependency of the mean depth t_{ALBSF} of the Al BSF on the initial layer thickness of the Al rear side metallization (Fig. 6 and Table 3). This dependency has also been found in previous studies [6–8] and can be explained by a varying concentration gradient between Al and Si during the formation of the Al-Si-eutectic within the contact firing process [9]. The I-V-results of the four experimental groups confirmed the findings of the SEM analysis in principle (Table 4 and Fig. 7 to Fig. 10). Particularly open-circuit voltage V_{oc} increased significantly between group 1 and 3 due to the increasing depth of the Al BSF and thus reduced recombination losses on the rear side. Fill factor FF also revealed slight differences between the groups which are most likely caused by slight variations of the front side metallization. Short-circuit current density j_{sc} is comparable for all 4 groups as the same FSP front side metallization has been applied in one run. The measurement of the I-V-parameters showed a comparable conversion efficiency $\eta = 19.4\%$ for group 2 and 3 compared to the FSP references group 4 with $\eta = 19.3\%$. Solar cells of group 3 showed a strong bow due to a different thermal expansion of the thick Al layer and the Si wafer during the contact firing process.

Summarizing the results it could be shown that rotary screen printing technology is able to apply the rear side metallization for Al BSF solar cells with a comparable high quality as flatbed screen printing. In order to ensure a sufficient Al layer thickness and thus a sufficient Al BSF it is essential to choose an adequate cylinder screen mesh. Furthermore, the Al paste has to be modified slightly to ensure a good paste transfer and printing result. Using RSP technology instead of FSP, the throughput for the rear side metallization of Si solar cells could possibly be increased by the factor 3 to 4.

Table 4: I-V-results of experimental group 1 to 4.

Group	Mean short-circuit current density j_{sc} [mA/cm ²]	Mean open circuit voltage V_{oc} [mV]	Mean fill factor FF [%]	Mean conversion efficiency η [%]
1	37.5 ± 0.2	639.0 ± 3.0	80.4 ± 0.1	19.2 ± 0.2
2	37.5 ± 0.1	641.7 ± 0.7	80.6 ± 0.2	19.4 ± 0.1
3	37.5 ± 0.1	642.7 ± 0.4	80.2 ± 0.3	19.4 ± 0.1
4	37.6 ± 0.1	642.2 ± 0.5	80.0 ± 0.2	19.3 ± 0.1

Fig. 7: Short-circuit current density j_{sc} of group 1 to 4.Fig. 8: Open-circuit voltage V_{oc} of group 1 to 4.Fig. 9: Fill factor FF of group 1 to 4.Fig. 10: Conversion efficiency η of group 1 to 4.

3.2. Experiment 2: front side metallization of Al BSF solar cells

The minimum line width on cylinder screens for graphic applications is usually limited to $w \geq 100 \mu\text{m}$. Yet, the front side metallization of Si solar cells typically requires line widths of $w_f = 50 \mu\text{m}$ and below in order to print narrow contact fingers. Thus, a SEM analysis has been carried out to investigate the ability of the manufacturing process to realize such narrow lines on cylinder screens. Two cylinder screens with an identical mesh (325 wires/inch) and a different emulsion layer has been fabricated with finger widths down to $w_n = 25 \mu\text{m}$. The quality of the printing channel for the finger elements have been analyzed by SEM. The results showed that channels down to a nominal width of $w_n = 25 \mu\text{m}$ could be reproduced precisely with both cylinder screens (Fig. 11). A slightly higher width of the channels compared to the nominal width w_n in the digital data could be traced back to a deviation of the finger width within the positive film which had been used to expose the cylinder screens with UV light. However, cylinder screen A revealed a significantly better quality of the channels. Within the channels of

screen B, thread-like filaments and residues of the emulsion layer could be observed. Thus, a cylinder screen type A had been chosen for the printing experiment.

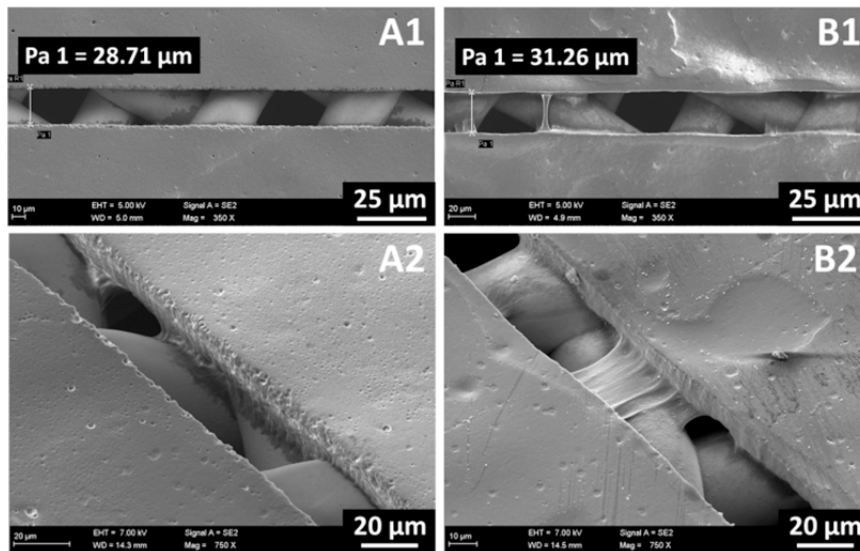


Fig. 11: SEM images of channels for contact finger elements within cylinder screens of type A (A1 and A2) and B (B1 and B2) (SEM parameters: secondary electron detection, accelerating voltage $V = 5.0 - 7.0$ KV, working distance $w = 4.9 - 14.5$ mm).

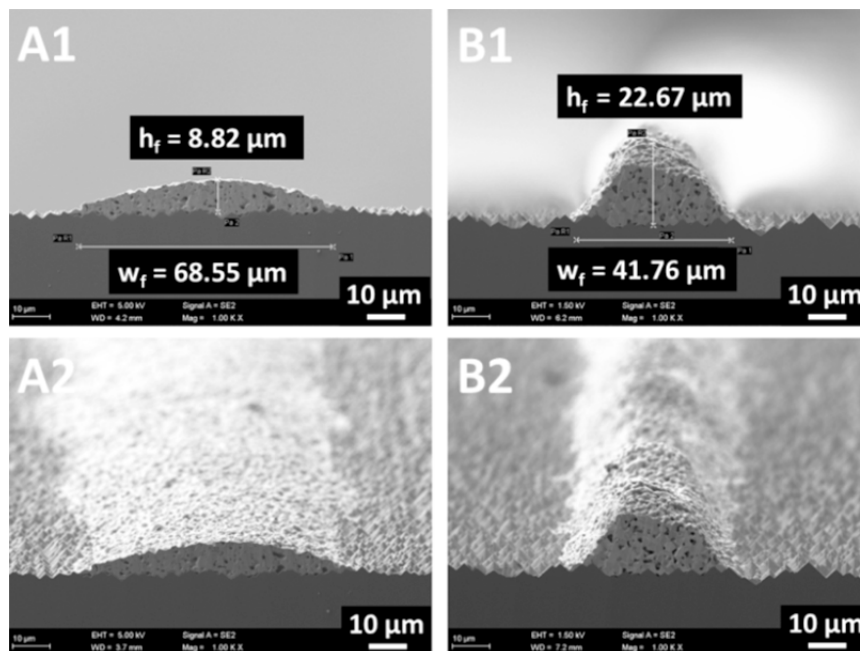


Fig. 12: SEM images of contact fingers printed with RSP within group 5 (A1 and A2) and FSP within group 6 (B1 and B2) (SEM parameters: secondary electron detection, accelerating voltage $V = 1.5 - 5.0$ KV, working distance $w = 3.7 - 7.2$ mm).

Table 5: Geometry of finger elements printed with RSP (group 5) and FSP (group 6)

Group	Nom. Finger width w_n [μm]	Mean finger width w_f [μm]	Mean finger height h_f [μm]	Mean finger cross-section area A_f [μm^2]	Mean lateral finger resistance R_L [Ω/cm]
5	25	61 ± 4	4 ± 1	149 ± 10	3.6 ± 0.3
	35	75 ± 11	6 ± 1	321 ± 56	1.9 ± 0.2
	45	86 ± 10	8 ± 2	442 ± 45	1.1 ± 0.1
6	40	42 ± 2	25 ± 2	794 ± 64	0.6 ± 0.1

A first printing test using RSP with a standard Ag paste revealed the necessity to modify the viscosity of the paste. By adding an amount of 6.4 wt% of a suitable thinner, the viscosity of the Ag paste was adjusted to $\eta = 0.7$ Pas (shear rate $\dot{\gamma} = 1000 \text{ s}^{-1}$). Further measurements also showed that the yield stress τ_y of the paste has been strongly reduced from $\tau_{y,\text{Orig}} = 3200$ Pa to $\tau_{y,\text{mod}} = 13$ Pa by the dilution. Using this modified paste, the test layout could be printed on Cz-Si precursors without visible interruptions. A profound investigation of the contact finger geometry has been carried out after drying and contact firing of the metallized precursors. The results showed significantly different finger geometries of both technologies (Table 5 and Fig. 12). Contact fingers printed with FSP (group 6) had a relatively high aspect ratio (height-to-width-ratio) with a mean finger width of $w_f = 42 \mu\text{m}$ and a finger height of $h_f = 25 \mu\text{m}$. Fingers printed with RSP showed a considerably flatter shape, a significantly broader mean finger width between $w_{f,\text{min}} = 61 \mu\text{m}$ and $w_{f,\text{max}} = 86 \mu\text{m}$. Finger height h_f was also considerably lower with $h_{f,\text{min}} = 4 \mu\text{m}$ to $h_{f,\text{max}} = 8 \mu\text{m}$. This led to an effective cross-section area A_f which is approx. 2 – 5 times lower compared to FSP contact fingers. Thus, RSP fingers of group 5 also revealed a higher mean lateral finger resistance of $R_L = 1.9 \Omega/\text{cm}$ compared to FSP fingers of group 6 with $R_L = 0.6 \Omega/\text{cm}$. The considerably flatter profile of the RSP fingers is most likely caused by two reasons: The lower viscosity η and the significantly lower yield stress τ_y of the diluted Ag-paste led to a stronger spreading of the paste during the printing process. Pospischil [10] and Kraft [11] found a particularly strong impact of the yield stress τ_y on contact finger geometry. Thus, a simple dilution of the Ag-paste is probably not optimal for a good contact finger geometry. It might thus be necessary to adjust the viscosity of the paste without reducing the yield stress too much. This could possibly be achieved by a modification of the organic matrix.

The main reason for the lower finger height h_f of RSP-printed fingers is the significantly lower paste transfer capability of cylinder screens. This is caused by a significantly higher wire thickness of such screens which is required due to stability reasons of the cylinder screen (Fig. 1).

Summarizing the results it can be stated that RSP technology is able to transfer an uninterrupted H-pattern grid on Cz-Si precursors using a modified Ag paste. However, the finger geometry is not optimal and has to be optimized with respect to finger width w_f and finger height h_f . A possible path to achieve this goal is the rheological optimization of the Ag paste with respect to viscosity η and yield stress τ_y .

4. Conclusion

Within this study, two separate experiments have been carried out. Experiment 1 investigated the ability of rotary screen printing technology to realize a rear side metallization of Al BSF solar cells with comparable I-V-results to a flatbed screen printing rear side metallization. The results of this experiment showed that a homogeneous Al rear side metallization could be successfully applied on Cz-Si precursors using RSP and a slightly diluted, commercially available Al paste. A SEM investigation revealed that the layer thickness of the RSP rear side metallization strongly depends on the used cylinder screen mesh. It could be further shown that the depth of the Al BSF depends on the initial Al layer thickness of the rear side metallization. Using a cylinder screen with 200 wires/inch led to a layer thickness of $d_{\text{Al,FFO}} = 20 \mu\text{m}$ which proved to be too low to form an Al BSF with a sufficient depth. Using a cylinder screen with 145 wires/inch led to an Al layer thickness of $d_{\text{Al,FFO}} = 26 \mu\text{m}$ (group 2) which was comparable to the

FSP reference (group 4) with $d_{\text{Al,FFO}} = 24 \mu\text{m}$. This group also obtained a mean Al BSF depth of $t_{\text{ALBSF}} = 3.6 \mu\text{m}$ which was comparable to the FSP reference group with $t_{\text{ALBSF}} = 4.0 \mu\text{m}$. Printing the rear side metallization with a high-capacity cylinder screen (88 wires/inch) resulted in a significantly higher layer thickness of $d_{\text{Al}} = 40 \mu\text{m}$. This led to significantly deeper Al BSF ($t_{\text{ALBSF}} = 7.8 \mu\text{m}$) but also caused a very strong bow of the solar cells after contact firing. The best I-V-results could be achieved with solar cells of group 2 and 3 (RSP-printed rear side metallization) with a conversion efficiency of $\eta = 19.4 \%$. FSP-printed reference cells achieved a mean conversion efficiency of $\eta = 19.3 \%$. Considering minor differences of the FF due to variations of the front side grid, comparable I-V-results could be achieved with both technologies. Summarizing the results it could be demonstrated that a rear side metallization of Al BSF solar cells can be realized with high-throughput rotary screen printing technology with the same quality as flatbed screen printed solar cells.

Within experiment 2, we investigated the ability of RSP technology to realize the front side metallization of Si solar cells. It was shown that a visually uninterrupted front side grid can be printed on Cz-Si precursors using RSP and a slightly diluted, commercially available Ag paste. Using RSP, finger with a mean width from $w_{f,\text{min}} = 61 \mu\text{m}$ to $w_{f,\text{max}} = 86 \mu\text{m}$ were realized depending on the nominal finger width w_n . Mean finger heights between $h_{f,\text{min}} = 4 \mu\text{m}$ and $h_{f,\text{max}} = 8 \mu\text{m}$ were achieved. The FSP-printed fingers obtained a significantly smaller mean finger width of $w_f = 42 \mu\text{m}$ and a greater mean finger height of $h_f = 25 \mu\text{m}$. Thus, FSP-printed fingers achieved a lower lateral finger resistance of $R_L = 0.6 \Omega/\text{cm}$ compared to RSP-printed fingers with R_L between $3,6 \Omega/\text{cm}$ and $1.1 \Omega/\text{cm}$. The flat finger profile of the RSP-printed fingers is most likely caused by a stronger spreading of the fingers during the printing process due to a lower viscosity η and a significantly smaller yield stress τ_y of the diluted Ag paste. The significantly thicker wires of the RSP cylinder screens further led to a lower paste transfer capacity and thus to a smaller finger height h_f . A promising path for a further optimization of an RSP-printed front side metallization could be a rheological optimization of the Ag paste (i.e. organic matrix) in combination with an optimized screen mesh for fine line printing.

Acknowledgements

This work was partly supported by the German Federal Ministry of Education and Research (BMBF) within the funding program Photonics Research Germany under the contract number 13N13512 (Rock-Star).

References

- [1] ASYS Group, Metallization Lines. http://www.asys.de/agweb/en/products-solutions/01_mettallization/ [Last access: 27.01.2017].
- [2] Kipphan H. Handbook of Print Media: Technologies and Production Methods, Heidelberg: Springer Science & Business Media; 2001
- [3] Lorenz A, Gredy C, Lehner M, Greutmann R, Brocker H, Rohde J, Senne A, Strauch T, Reinecke H, Clement F. Progress with Rotational Printing for the Front Side Metallization of Silicon Solar Cells. Proc. of the 32nd EUPVSEC 2016; p. 413–9.
- [4] Hahne P. Innovative Druck- und Metallisierungsverfahren für die Solarzellentechnologie. PhD Thesis 2000; Fernuniversität Hagen.
- [5] Strauch T, Demant M, Lorenz A, Haunschild J, Rein S. Two Image Processing Tools to Analyse Alkaline Texture and Finger Geometry in Microscope Images. Proc. of the 29th EUPVSEC 2014; p. 1132-7.
- [6] del Alamo J, Eguren J, Luque A. Operating limits of Al-alloyed high-low junctions for BSF solar cells. Solid-State Electronics 1981; 24:24: p. 415–420.
- [7] Aijuan G, Famin Y, Lihui G, Dong J, Shimeng F. Effect of the back surface topography on the efficiency in silicon solar cells. J. Semicond. 2009; 30: p. 074003
- [8] Kaminski A, Vandelle B, Fave A, Boyeaux J, Le Nam Q, Monna R, Sarti D, Laugier A. Aluminium BSF in silicon solar cells. Solar Energy Materials and Solar Cells 2002; 72: p. 373–9.
- [9] Seith W. Diffusion in Metallen: Platzwechselreaktionen. Berlin, Heidelberg: Springer; 1955.
- [10] Pospischil M. A Parallel Dispensing System for an Improved Front Surface Metallization of Silicon Solar Cells. PhD Thesis 2016. Albert-Ludwigs-Universität Freiburg.
- [11] Kraft A. Plated Copper Front-Side Metallization on Printed Seed-Layers for Silicon Solar Cells. PhD Thesis 2015; Albert-Ludwigs-Universität Freiburg.